Journal of Natural Sciences Research www.iiste.org
ISSN 2224-3186 (Paper) ISSN 2225-0921 (Online)
Vol.5, No.7, 2015

Analysis of a Non-Reacting Laminar Fluid Flow with Viscous Dissipation through a Porous Channel Formed by Two Parallel Horizontal Permeable Walls

Olaseni Taiwo Amumeji
Department of Mathematical Science, Ondo State University of Science and Technology, P.M.B. 535, Okitipupa,Ondo State, Nigeria

Abstract
The analytical solutions for the steady momentum and heat transfer of a non-reacting Newtonian viscous incompressible laminar fluid flow in a channel filled with saturated porous media with isothermal and isoflux heating walls were reported. The problem was studied under the viscous dissipation and suction/injection. The effects of various emerging parameters involved in the steady solution of the problem are discussed using contour graphs. It was revealed that with the imposition of suction/injection ($Re \neq 0$) on the walls, the velocity close to the wall suction of the channel increases faster as compared to the opposite wall injection as Da increases as well as the ratio of viscosities M decreases. It was further shown that the fluid temperature is more influenced in isothermal process if either the Darcy number Da, or Brinkman number Br, or wall suction Reynolds number, Re or the three parameters are increased and either the ratio of viscosity M, or Peclet number Pe, or the wall injection Reynolds number, Re or the three parameters are decreased. With the same imposition in isoflux heating process, the fluid temperature distribution is more enhanced with increase in values of Pe or Br and decrease in values of M or wall suction/injection Reynolds numbers Re or the two emerging parameters respectively, while the effect of Darcy number Da on the flow results in an anomalous phenomenon in temperature distribution in the presence of suction Reynolds number Re.
Keywords: laminar flow, non-reacting fluid, suction/injection, isothermal, isoflux

1. Introduction

Considerable attention has been given to the study of transport phenomena in a laminar flow in the channel filled with saturated porous media by the scientists, engineers and experimentalists in recent years because it is often observed in the field of electronics cooling system, solid matrix heat exchanger, geothermal system, nuclear waste disposal, microelectronics heat transfer equipment, coal and grain storage, petroleum industries, and catalytic converters. Convective heat transfer through a porous media has been a subject of great interest for the last three decades. The problems of natural convection flow through porous medium past a plate had been solved (Kim and Vafai 1989 and Harris, Ingham and Pop 1997). Also, the analytical solutions for unsteady free convection in porous media were discussed (Magyari, Pop and Keller 2004) while the magnetic current in porous media was considered (Raptis and Perdikis 1983 and Geindreau and Auriault 2002). The flow of an incompressible viscous fluid past an infinite plate oscillating with increasing or decreasing velocity amplitude of oscillation was investigated (Turbatu, Buhler, and Zierep 1998). On the other hands, flow through porous medium have numerous engineering and geophysical applications processes, for example, in chemical engineering for filtration and purification; in agriculture to study the underground water resources; in petroleum technology to study the movement of natural gas, oil and water through the soil reservoirs. In view of these applications, many researchers have studied this area with keen interest (Raptis and Kafoussias 1982, Sattar 1993 and Kim 2004).

For the fluids, which are important in the theory of lubrication, the heat generated by the internal friction and the corresponding rise in temperature do affect the thermal conductivity of the fluid. The investigation of the effect of temperature dependent viscosity and thermal conductivity on the unsteady MHD convective heat transfer past a semi-infinite vertical porous moving plate with variable suction had been carried out (Saddeek and Salama 2007) while the variable viscosity and thermal conductivity on the heat and mass transfer characteristics in mixed convection about a wedge in saturated porous media was studied (Hassanien, Essawy and Moursy 2003). It was discussed that the process of suction and blowing also has its importance in many engineering activities (Labropulu, Dorrepaal and Chandna 1996) such as in the design of thrust bearing and radial diffusers, and thermal oil recovery. Suction is applied to chemical processes to remove reactants. Blowing is used to add reactants, cool the surface, prevent corrosion or scaling and reduce the drag. Also, the heat transfer characteristics of a steady, incompressible, magneto-micropolar fluid flowing past an isothermal stretching sheet with suction and blowing through a porous medium in the presence of radiation and variable viscosity was studied (Elbarbary and Elgazery 2004). The unsteady free convection and mass transfer boundary layer flow past an accelerated infinite vertical porous flat plate with suction was considered (Dass, Mohanty, Panda and Sahoo 2008) when the plate accelerates in its own plane. The governing equations are solved both

analytically and numerically using finite difference scheme. It was shown that the flow phenomenon was characterized with the help of flow parameters such as suction parameter, porosity parameter, Grashof number, Schmidt number and Prandtl number and their effects on velocity, temperature and concentration distributions are also studied. In many practical and experimental circumstances, free convection flows are generated adjacent to surfaces dissipating heat at a prescribed heat flux rate. Exact solutions of incompressible Couette flow with constant temperature and constant heat flux on walls was studied (Chaudharcy and Jain 2007) in the presence of radiation. Their paper investigated a closed form solution for the transient free convection flow of a viscous fluid between two infinite vertical parallel plates in the presence of radiation. The flow is set up due to free convective currents occurring as a result of application of constant heat flux (CHF) at one wall and constant temperature on the other wall. The governing partial differential equations have been solved exactly using the Laplace-transform technique. The numerical values obtained from analytical expressions of velocity, temperature, skin-friction, and Nusselt number have been presented graphically to study the behaviour of flow on momentum and thermal boundary layer.

The study of the effects of nth order Arrhenius chemical reaction, thermal radiation, suction/injection and buoyancy forces on unsteady convection of a viscous incompressible fluid past a vertical porous plate was carried out (Makinde, Olanrewaju and Charles 2011). Their results revealed among others things that the fluid velocity within the boundary layer decreases with increasing values of buoyancy forces and wall suction, and increases with wall injection. The temperature profile decreases in the presence of radiation absorption and increases with increasing rate of exothermic chemical reaction and reaction order. In addition, the chemical species concentration within the boundary layer increases with increasing reaction and wall injection.

In all the above mentioned works, none was found to study the laminar flow of a non-reacting fluid with viscous dissipation within a porous channel with two distinct horizontal permeable wall conditions, hence the motivation.

2. MATHEMATICAL FORMULATION

We present in this work, the set of dimensional non-linear ordinary differential equations describing a Newtonian viscous incompressible laminar flow with two distinct boundary conditions in the mathematical models. We consider momentum and heat transfer equations by laminar flow for the steady state hydro-dynamically and thermally developed situations which have unidirectional flow of a viscous combustible non-reacting Newtonian fluid in the x-direction between permeable boundaries at $\bar{y}=0$ *and* $\bar{y}=a$ as in figure 1. The channel is composed of a lower heated wall with surface constant temperature (isothermal) or constant heat flux (isoflux) while the upper wall is isothermal. We follow closely and modify the models presented in Lamidi and Ayeni [10].

In the following sections, the dimensionless non-linear steady-state momentum and energy balance equations, which govern the problem is obtained as follows.

The continuity equation is given as

$$\frac{d\bar{v}}{d\bar{y}}=0 \tag{1}$$

The Brinkman momentum equation with its boundary conditions is

$$\rho\bar{v}\frac{d\bar{u}}{d\bar{y}}=\mu_e\frac{d^2\bar{u}}{d\bar{y}^2}-\frac{\mu}{K}\bar{u}+G,\quad \bar{u}(0)=0,\ \ \bar{u}(a)=0 \tag{2}$$

The dimensionless form of equation (2) is

$$M\frac{d^2u}{dy^2}-\mathrm{Re}\frac{du}{dy}-\frac{u}{Da}=-1,\qquad u(0)=0,\ u(1)=0 \tag{3}$$

The steady-state energy equation for the problem is given as

$$\rho c_p\bar{v}\frac{dT}{d\bar{y}}=k\frac{d^2T}{d\bar{y}^2}+\mu\left(\frac{d\bar{u}}{d\bar{y}}\right)^2 \tag{4}$$

with the following boundary conditions

$$T=T_0 \text{ or } \frac{dT}{d\bar{y}}=-\frac{q}{k} \text{ at } \bar{y}=0 \text{ and } T=T_0 \text{ at } \bar{y}=a \tag{5}$$

The dimensionless form of equations (4) and (5) are respectively given as

$$\frac{d^2\theta}{dy^2} - Pe\frac{d\theta}{dy} + Br\left(\frac{du}{dy}\right)^2 = 0, \tag{6}$$

And

$$\theta = 0 \text{ or } \frac{d\theta}{dy} = -1 \text{ at } y = 0 \text{ and } \theta = 0 \text{ at } y = 1, \tag{7}$$

where in the case described above $a, Br, c_p, Da, G, k, K, M, Pe, q, \mathrm{Re}, T_0, T, u, \bar{u}, \bar{v}, \bar{y}, \mu, \mu_e, \rho, \theta$ are defined in the nomenclature.

The $\bar{x}$ -axis is along the wall and in the horizontal direction and the $\bar{y}$ - axis normal towards it. The fluid is Newtonian, viscous and incompressible.

The equation of continuity in (1), on integration, gives $\bar{v} =$ constant (V_0 , say) is the normal velocity of suction or injection at the walls accordingly as $V_0 < 0$ or $V_0 > 0$ (permeable walls) respectively as against $V_0 = 0$ (Lamidi and Ayeni [10]) which represents the case of impermeable walls. The channel's walls are uniformly porous.

In order to unify the isothermal heating and isoflux heating at one condition, we may write

$$\theta = 0 \text{ or } \frac{d\theta}{dy} = -1 \text{ to } A\frac{d\theta}{dy} + B\theta = C \text{ at } y = 0 \tag{8}$$

and

$$\theta = 0 \text{ at } y = 1, \tag{9}$$

where *A, B* and *C* are constants depending on the isothermal heating or isoflux heating.
For the isothermal heating: $A = 0$, $B = 1$ and $C = 0$
while for isoflux heating: $A = 1$, $B = 0$ and C = -1

3.METHOD OF SOLUTION

The method of undetermined coefficients was used in solving the governing momentum and energy equations. In addition, the summary of the result together with the corresponding contour graphical representation were obtained using the symbolic algebraic computer programming software packages namely MAPLE and MATLAB.

Now, using the method of undetermined coefficients, the solution of (3) could be easily obtained as

$$u(y) = b_1 e^{r_1 y} + b_2 e^{r_2 y} + Da, \tag{10}$$

where

$$r_1 = \frac{R_e + \sqrt{R_e^2 + \frac{4M}{Da}}}{2M}, \quad r_2 = \frac{R_e - \sqrt{R_e^2 + \frac{4M}{Da}}}{2M}, \quad b_1 = -\frac{Da(e^{r_2\lambda} - 1)}{e^{r_2\lambda} - e^{r_1\lambda}}, \quad b_2 = \frac{Da(e^{r_1\lambda} - 1)}{e^{r_2\lambda} - e^{r_1\lambda}}$$

Now, using (10) in (6) we have

$$\frac{d^2\theta}{dy^2} - Pe\frac{d\theta}{dy} = -Br\left(r_1 b_1 e^{r_1 y} + r_2 b_2 e^{r_2 y}\right)^2 \tag{11}$$

Solving for homogeneous and particular parts to get the general solution using the method of undetermined coefficients, we have

$$\theta(y) = \theta_c(y) + \theta_p(y)$$

i.e

$$\theta(y) = b_3 + b_4 e^{y(r_1 + r_2)} + b_5 (b_6 e^{2r_1 y} + b_7 e^{2r_2 y} + b_8 b_9 e^{Pe\, y}), \tag{12}$$

where

$$b_3 = (b_{10}\, e^{\lambda(r_2+r_1)} - b_{11}\, e^{2r_2\lambda} - b_{12} e^{2r_1\lambda} - b_{13} e^{Pe\lambda})b_{14},$$

$$b_4 = \frac{2Brr_1^2 r_2^2 b_1 b_2}{(r_1+r_2)(Pe-r_1-r_2)},\quad b_5 = \frac{1}{(Pe-2r_1)(Pe-2r_2)},\quad b_6 = \frac{1}{2} Brr_2^3 b_2^2 (Pe-2r_1),$$

$$b_7 = \frac{1}{2} Brr_1^3 b_1^2 (Pe-2r_2),\quad b_8 = -(b_{15} - b_{16} e^{\lambda(r_1+r_2)} - b_{17} e^{2r_2\lambda} - b_{18} e^{2r_1\lambda})b_{19},$$

$$b_9 = \frac{(Pe-2r_2)(Pe-2r_1)}{Pe},\quad b_{10} = -b_4(B+APe),\quad b_{11} = b_5 b_6 (APe+B),$$

$$b_{12} = b_5 b_7 (APe+B),\qquad b_{14} = \frac{1}{APe + B(1-e^{Pe\lambda})},$$

$$b_{13} = -Ab_4(r_2+r_1) - b_5 b_7 (2Ar_1+B) - b_5 b_6 (2Ar_2 - B) - Bb_4 + C,$$

$$b_{15} = Ab_4(r_2+r_1) + b_5 b_6 (2Ar_2+B) + b_5 b_7 (2Ar_1+B) + Bb_4 - C,$$

$$b_{16} = Bb_4,\quad b_{17} = Bb_5 b_6,\quad b_{18} = Bb_5 b_7,\quad b_{19} = \frac{1}{b_5 c_9 (APe + B(1-e^{Pe\lambda}))},$$

4 RESULTS AND DISCUSSION

Velocity Profile

The dimensionless steady velocity distributions of the non-reacting laminar fluid flow in the channel filled with saturated porous media with the imposition of wall suction/injection are illustrated in the contour graphs of figures 2 to 6 to reveal the influence of the emerging parameters in equation (10).

It is revealed in figure 2, that the velocity profile of the fluid increases as *Da* increases due to the decrease in the inhibitive influence of the permeability parameter in both cases of suction and blowing hence the fluid flows quickly. It is also shown that the dimensionless velocity close to the suction wall of the channel increases faster as compare to the opposite injection wall as *Da* increases with the imposition of suction Reynolds number (*Re* = 5.0). In figure 3, it is observed that the imposition of suction/injection Reynolds number has no significant effects on the fluid velocity for all values of viscosity ratio when the permeability is very small as observed in Lamidi and Ayeni [10], This implies that the presence of suction/injection on the wall is insignificant in aiding or altering the flow at a very low Darcy number (below 10^{-3}).

In figure 4, the velocity is observed to decrease as *M* increases at higher Darcy number (*Da* = 0.1) in the presence of suction/injection Reynolds number (*Re* = 5). This is physically true since an increase in viscosity ratio is achieved by a decrease in the fluid viscosity which eventually leads to a decrease in fluid velocity as shown in figure 4, however, it was noticed that the flow decays faster towards the suction wall. Figures 5 and 6 show the influences of wall suction/injection Reynolds numbers on fluid velocity within the channel. Figure 5 depicts the influence of injection $(\mathrm{Re} < 0)$ on the flow velocity in the boundary layer. It is revealed that imposition of wall fluid injection increases the hydrodynamic boundary layer which indicates an increase in the fluid velocity. However, the exact opposite behaviour is observed by the imposition of wall fluid suction $(\mathrm{Re} > 0)$ in figure 6. As it is vividly observed in figure 5, the velocity profile rises as it moves away from the injection wall, while in figure 6, as the suction Reynolds number increases; the maximum fluid velocity is monotonically decreasing indicating the usual fact that suction stabilizes the boundary layer growth. This can be physically interpreted by the fact that the suction is to take away the warm solute on the wall thereby decreasing the velocity with a reduction in the intensity of the natural convection rate. It is evident here that the effect of suction is to decrease the velocity and that of blowing is to increase the velocity. These results are consistent with the physical situation.

Temperature Profile

A graphical representation of the numerical results is illustrated in figures 7 through 25 to show the influence of the Darcy number, *Da*, Ratio of viscosities, *M*, Peclet number, *Pe*, Brinkman number, *Br* and suction/injection Reynolds number, *Re* on a non-reacting fluid flow of equation (12) in the saturated porous channel with the two

distinct horizontal thermal boundary conditions - isothermal and isoflux processes. Figures 7 to 11 depicts the influence of Darcy number *Da* and ratio of viscosities *M* on the flow temperature profile. In figure 7 with isothermal process, temperature is observed to increase as *Da* increases. In addition, another observation from this figure shows a sharp decay in the fluid temperature near the suction wall in comparison to the gentle decay near the wall with injection. This is physically true since the wall suction takes away the warm solute on the wall thereby causing decay in the temperature of the fluid towards the plate. Also, temperature increase due to the growth of Darcy number is as a result of velocity increase which increases the viscous dissipation and hence the fluid temperature.

In figure 8 with isoflux boundary conditions, it was shown that the temperature profile is independent of the Darcy number. This agrees with the result of Lamidi and Ayeni [10] where the suction/injection effect is absent. Temperature profile in figure 9 show-cases the effect of ratio of viscosities, *M*, in the case of suction/injection walls with isothermal boundary condition. Here, the temperature is described as a decreasing function of the ratio of viscosities, *M*. From this figure, it is observed that the temperature is higher near the heated wall when *M* is very small. This is because as the suction/injection of the fluid through the channel wall increases, the wall is cooled down and in consequence, the viscosity of the flowing fluid increases. Therefore, there is a gradual decrease in fluid temperature as well as fluid velocity when compared with Lamidi and Ayeni [10].

In the case of figure 10 with isoflux process, increase in *M* also causes a steady attainment in fluid temperature due to the imposition of wall suction. It is also noticed that at a relatively higher values of *M*, the dependence of temperature on *M* is observed to decrease with it. This is because the fluids with large ratio of viscosities *M*, have low thermal diffusivity which causes low heat penetration and a reduced thermal boundary layer. Figure 11 shows the simultaneous effects of Darcy number, *Da* and ratio of viscosities, *M* for isothermal boundary condition, this confirms that the temperature increases with increase in Darcy number while it decreases with increase in ratio of viscosities *M*.

It is further shown in the case of isoflux boundary condition in figure 12, the simultaneous effects of the Darcy number, *Da* and ratio of viscosities, *M* in the presence of suction/injection Re, here it is displayed that the temperature decreases with increase in ratio of viscosities, *M* whereas an anomalous phenomenon is noticed as *Da* increases. It is seen that the temperature profile initially exhibits the usual behaviour of increasing as *Da* increases before finally decreases with increase in *Da*. The range of *Da* for which this anomalous phenomenon is noticed depends on the value of suction Reynolds number ($Re = 5.0$). This is expected since $Re >> Da$ means that suction exerts a greater influence on temperature. Such an anomalous phenomenon is not observed in the absence of wall suction/injection (Lamidi and Ayeni [10]).

The temperature of the flow field is affected by the variation of Peclect number, *Pe* in the presence of wall suction/injection. In both isothermal and isoflux cases, these variations are shown in figures 13 and 14 respectively. Figure 13 is a plot of temperature fields within the channel for different values of Peclet number, *Pe*. This figure displays that the Peclet number decreases the temperature at all points of the flow fields with the usual trend of faster decay of the temperature near the suction wall. With the increase in Peclet number, the thermal conduction in the flow is lowered and the viscosity of the flowing fluid becomes higher. In consequence, the molecular motion of the fluid elements is lowered therefore the flow field suffers a decrease in temperature as Peclect number is increased. It is also discovered in this figure that the imposition of wall suction reduces the rate of decrease in fluid temperature with increase in *Pe*.

In figure 14, a contrary view to figure 13 is also noticed, in the case of isoflux heating. It is shown that the fluid temperature is an increasing function of Peclet number, *Pe*. It is presented in figure 15 for isothermal heating process that, the fluid temperature increases with an increase in Brinkman number *Br*, but the temperature field is enhanced near the wall suction at a higher *Br*. This explains that the dimensionless temperature close to the wall suction increases as Brinkman number increases. In the case of isoflux heating process, in figure 16, the fluid temperature increases as *Br* increases and is higher near the wall injection of the channel. This investigated the effect of viscous dissipation in the presence of suction/injection walls with isoflux process that the dimensionless temperature is greater nearer the wall injection as Brinkman number increases. It is also revealed that the temperature is fast becoming steadier at a lower temperature near the wall with suction in the channel. The simultaneous effects of *Br* and *M* on the temperature profile in the case of isothermal and isoflux boundary conditions are respectively displayed in figures 17 and 18, these clearly show that temperature profiles increase with increase in *Br* and decrease in *M*.

In figures 19 to 25, the contour graphs present the variations in the dimensionless temperature of the flow field due to the change of suction/injection Reynolds number, *Re* keeping other parameters of the flow field constant. Figures 19 to 22 display the variation of temperature due to fluid blowing (figures 19 and 20) and suction (figure 21 and 22) in an isothermal and isoflux cases respectively. In figure 19, it is displayed that the fluid temperature decreases with increase in wall injection *Re*. It is further seen that there is a gentle decay in temperature near the wall with injection. This indicates that the thermal boundary layer thickness decreases as

injection *Re* increases. The action of fluid injection is to fill the space immediately adjacent to the wall with fluid having nearly the same temperature as that of the wall, thus the injected flow forms an effective insulating layer by decreasing the heat transfer from the channel wall. It is noted that blowing (injection) retards the flux of heat to the wall injection, thus as expected, blowing causes a reduction in heat transfer, as a result of this, the temperature decreases with increase in the wall injection (figure 20).

It is observed in figure 21, that the temperature is known to increase if suction rate increases. In addition, a sharp decay is discovered in the temperature field near the wall suction thus suction serves the function of bringing large quantities of ambient fluid into the immediate neighbourhood of the wall surface. As a consequence of the increased heat-consuming ability of this augment flow, the temperature drops quickly as we proceed away from the wall. It is also observed that increase in wall suction evidently decreases the temperature field of the fluid (figure 22). This is because as the suction of the fluid through the channel wall increases, the channel is cooled down and in consequence, there is a gradual decrease in fluid temperature. However the temperature becomes steadier near the wall suction.

Figures 23 and 24 show the simultaneous effects of blowing (injection) *Re* and ratio of viscosities, *M* on the temperature fields at a fluid section within the channel. From the figures, it is confirmed that temperature is a decreasing function of both emerging parameters in the isothermal as well as the isoflux cases. Finally, it is shown in the case of isoflux boundary condition in figure 25, the simultaneous effects of the suction Reynolds number, *Re* and ratio of viscosities, *M*, confirmed here that the temperature profile decreases with increase in suction Reynolds number, *Re* and ratio of viscosities, *M*.

5. CONCLUSION

The effects of suction/injection Reynolds number, Peclet number, Darcy number, Brinkman number and viscosity ratio on a non-reacting Newtonian viscous incompressible laminar fluid flow in a permeable channel filled with saturated porous media with horizontal isothermal and isoflux heating walls have been investigated. This study agrees well with the conclusion of Lamidi and Ayeni [10] and further concludes as follows:

1. The introduction of suction/injection has controlling and significant effects on the flow when the permeability is high thereby distorted the symmetric nature of the flow considered by Lamidi and Ayeni [10].
2. The effect of suction/injection is insignificant at a very low Darcy number *Da* as M increases.
3. The wall suction/injection Reynolds number, *Re* has more significant influence on the flow temperature near the walls of the channel in case of isothermal heating process in comparison to the isoflux cases.
4. The effect of Darcy number *Da* on the flow temperature distribution results in an anomalous phenomenon in the presence of suction Reynolds number *Re* in the case of isoflux heating process. The range of *Da* for which this anomalous phenomenon is noticed depends on the value of suction Reynolds number.
5. The effects of Peclet number on the flow temperature distributions in the channel are opposite in isothermal and isoflux heating cases.

Reference

Chaudharcy, R.C., and Jain, P. (2007) "Exact solutions of incompressible Coutte flow with constant temperature and constant heat flux on walls in the presence of Radiation", *Turkish Journal of Engineering, EMS Science,* 297-304.

Dass, S.S., Mohanty, M., Panda, J.P., and Sahoo, S.K. (2008) "Hydromagnetic couette flow and heat transfer", *Journal of Naval Architecture and Marine Engineering, ANAME Publication,* http://jname.8m.net.

Elbarbary, E.M.E., and Elgazery, N.S. (2004) *Int. Commun. Heat Mass Transfer*, 31, 409-419.

Geindreau, C., Auriault, J.L. (2002) "Magnetohydrodynamic flows in porous media", *J. Fluid Mech*., 466, 343–363.

Harris, S.D., Ingham, D.B., and Pop, I. (1997) "Free convection from a vertical plate in a porous medium subject to a sudden change in surface heat flux", *Transport in Porous media*, 26, 207–226.

Hassanien, I.A., Essawy, A.H., and Moursy, (2003) *Appl. Math. Comput*., 145, 667-682.

Kim, S.J., and Vafai, K. (1989) "Analysis of natural convection about a vertical plate embedded in porous medium", *Int. J. Heat Mass Transfer*, 32, 665–677.

Kim, Y.J. (2004) "Heat and mass transfer in MHD micropolar flow over a vertical moving porous plate in a porous medium" ,*Transport in Porous Media*, 56(1), 17–37.

Labropulu, F., Dorrepaal, J.M., and Chandna, O.P. (1996) "Oblique flow impinging on a wall with suction or blowing", *Acta Mech.,* 115, 15-25.

Lamidi, O.T, and Ayeni, R.O. (2012) "Analytical solution of a steady non-reacting laminar fluid flow in a channel filled with saturated porous media with two distinct horizontal impermeable wall conditions", *Journal of*

Natural Sciences Research, 2(3), 80-90.
Magyari, E., Pop, I., and Keller, B. (2004) "Analytic solutions for unsteady free convection In porous media", *J. Eng. Math*. .48, 93–104.
Makinde, O.D., Olanrewaju, P.O., and Charles, W.M. (2011) "Unsteady convection with chemical reaction and radiative heat transfer past a flat porous plate moving through a binary mixture". *Afr. Mat*. 22, 65-78.
Raptis, A., and Kafoussias, N.G. (1982) "Magnetohydrodynamic free convection flow and mass transfer through porous medium bounded by an infinite vertical porous plate with constant heat flux", *Can. J. Phys*., .60(12), 1725–1729.
Raptis, A., and Perdikis, C. (1983) "Unsteady free convection flow through a porous medium", *Energy Research*, 7, 391–395.
Saddeek, M.A., and Salama, F.A. (2007) *Comput. Mater. Sci.* 40, 186-192.
Sattar, M.A. (1993) "Unsteady hydromagnetic free convection flow with hall current mass transfer and variable suction through a porous medium near an infinite vertical porous plate with constant heat flux", *Int. J. Energy Research*, 17, 1–5.
Turbatu, S., Buhler, K., and Zierep, J. (1998) "New solutions of the 11 strokes problem for an oscillating flat plate", *Acta Mechanica*, 129, 25–30.

Nomenclature

We give the definition of the physical parameters that feature in this problem and except otherwise stated, these parameters will assume the definitions given.

a	channel width
c_p	specific heat at constant pressure
G	applied pressure gradient
k	fluid thermal conductivity
K	permeability of the porous mediu
q	fluid flux rate
T_o	wall temperature
T	absolute temperature
$\bar{u}$	fluid velocity
$\bar{v}$	normal velocity to the wall
V_0	suction velocity
$\bar{x}$	axial coordinate
$\bar{y}$	transverse coordinate

Greek Symbols

μ	fluid viscosity
μ_e	effective viscosity in the Brinkman term
ρ	fluid density

Dimensionless Group

$y = \frac{\bar{y}}{a}$	dimensionless transverse coordinate
$u = \frac{\mu \bar{u}}{Ga^2}$	dimensionless velocity
$v = \frac{\mu}{\rho}$	kinematic viscosity
$M = \frac{\mu_e}{\mu}$	ratio of viscosities
$Da = \frac{K}{a^2}$	Darcy number
$Br = \frac{G^2 a^3}{q\mu}$	Brinkman number

$Pe = \frac{\rho c_p V_0 a}{k}$ Péclet number

$\mathrm{Re} = \frac{\rho V_0 a}{\mu}$ dimensionless suction/injection Reynolds number

$\theta = \frac{k}{qa}(T - T_0)$ dimensionless temperature

Graphs

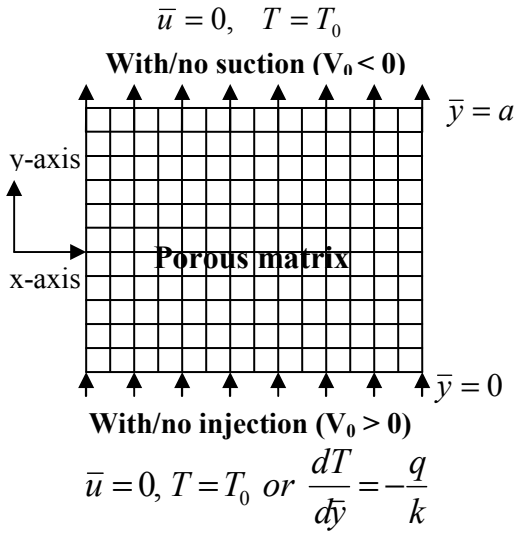

Figure 1: Problem Geometry

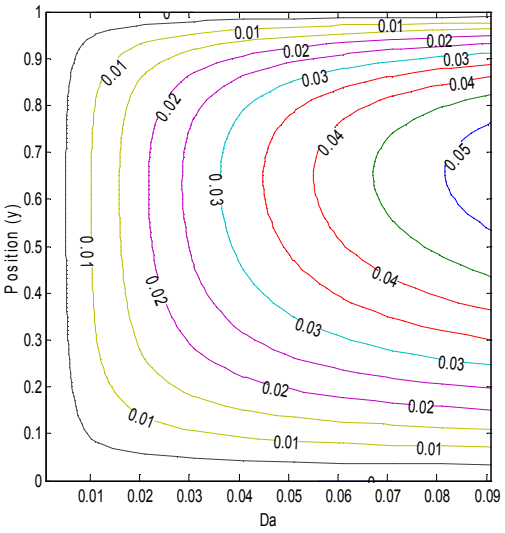

Figure 2: Contour Graph of velocity u(y) at various values of Da with Re = 5.0, M = 1.0 for equation (10)

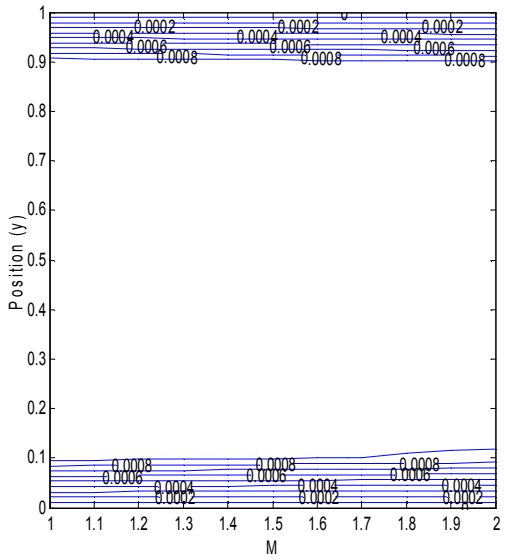

Figure 3: Contour graph of velocity u(y) at various values of M with Re = 5.0 Da = 0.001 for equation (10)

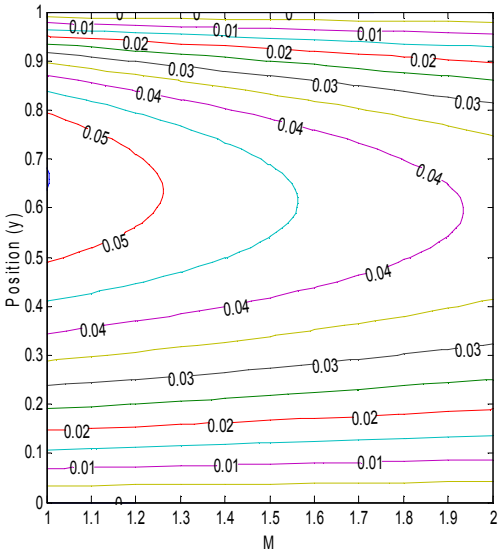

Figure 4: Contour graph of velocity u(y) at various values of M with Re = 5.0 Da = 0.1 for equation (10)

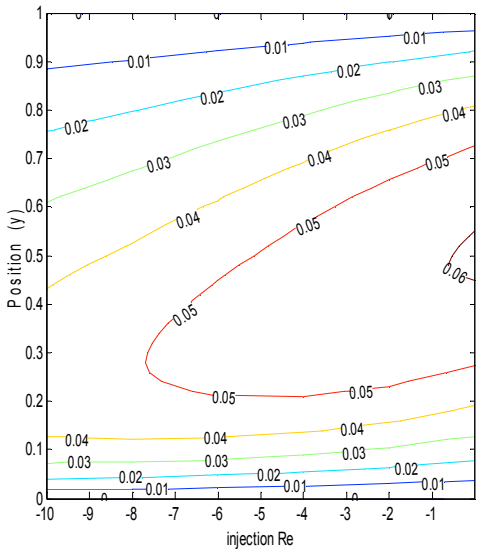

Figure 5: Contour graph of velocity u(y) at various values of injection Re with M = 1.0, Da = 0.1 for equation (10)

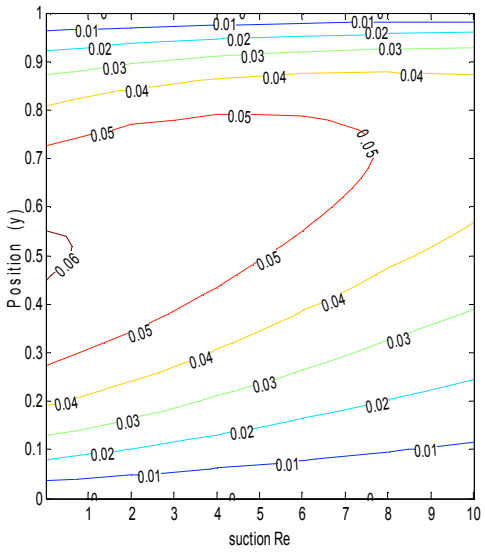

Figure 6: Contour graph of velocity u(y) at various values of suction Re with M =1.0, Da = 0.1 for equation (10)

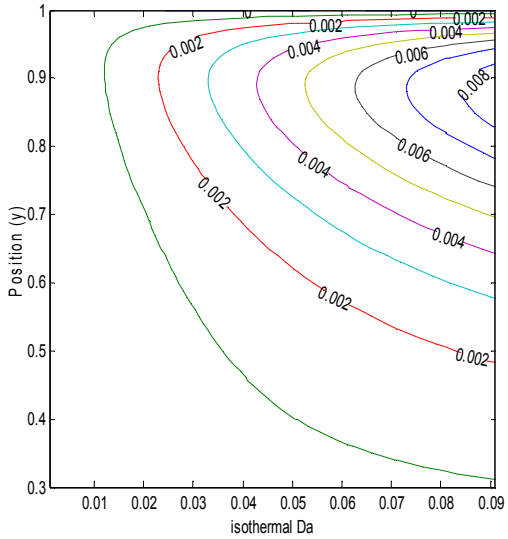

Figure 7: Contour graph of temperature θ(y) at various values of Da with Re = 5.0, Br = 0.3, Pe = 7.1, M = 1.0 (isothermal) for equation (12)

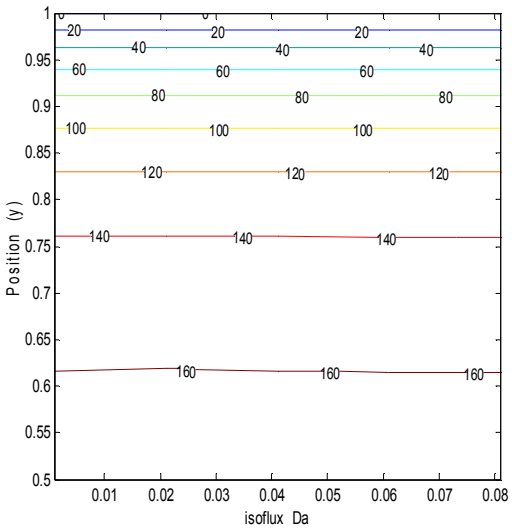

Figure 8: Contour graph of temperature θ(y) at various values of Da with Re = 5.0, Br = 0.3, Pe = 7.1, M = 1.0 (isoflux) for equation (12)

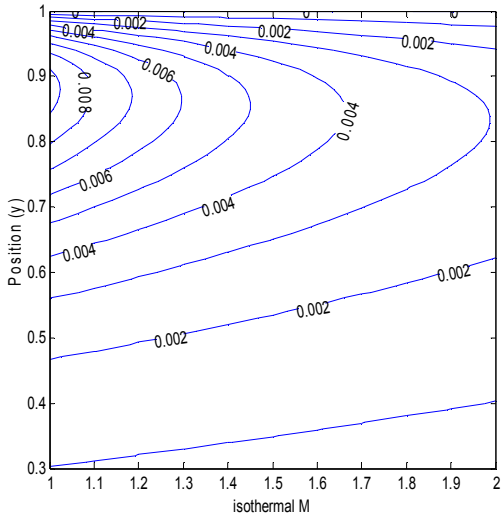

Figure 9: Contour graph of temperature θ(y) at various values of M with Re = 5.0, Br = 0.3, Pe = 7.1, Da = 0.1 (isothermal) for equation (12)

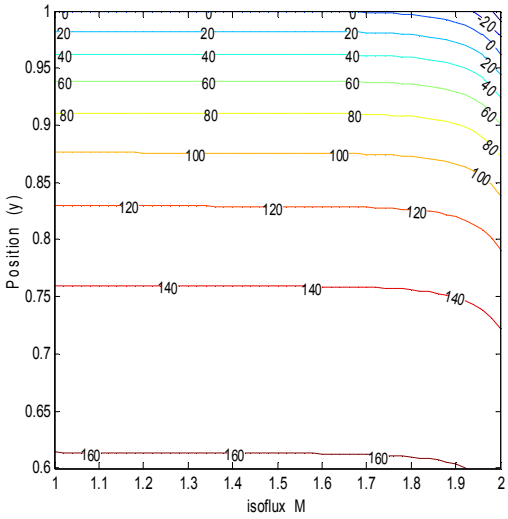

Figure 10: Contour graph of temperature θ(y) at various values of M with Re = 5.0, Br = 0.3, Pe = 7.1, Da = 0.1 (isoflux) for equation (12)

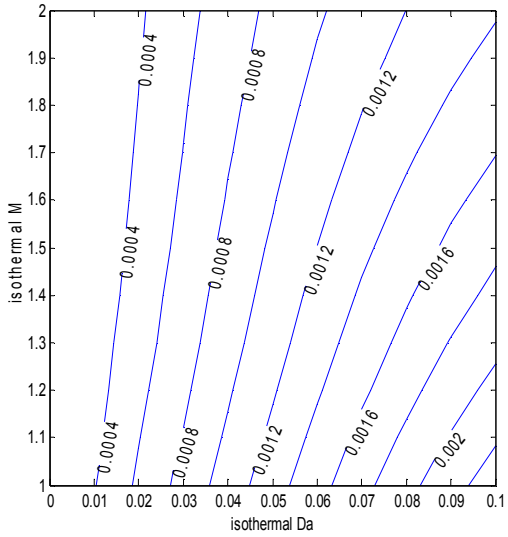

Figure 11: Contour graph of temperature θ(y) at various values of Da and M with Re = 5.0, Br = 0.3, Pe = 7.1, y = 0.5 (isothermal) for equation (12)

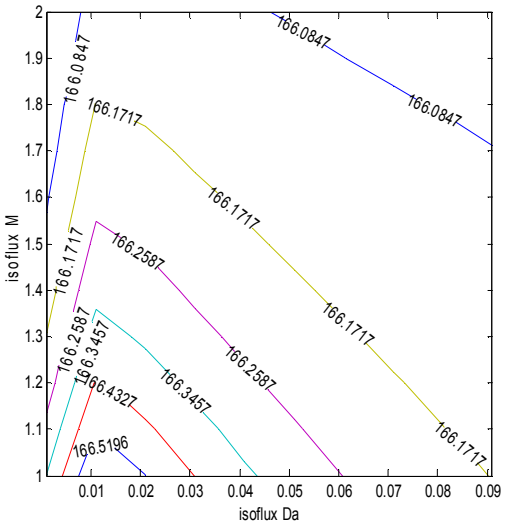

Figure 12: Contour graph of temperature θ(y) at various values of Da and M with Re = 5.0, Br = 0.3, Pe = 7.1, y = 0.5 (isoflux) for equation (12)

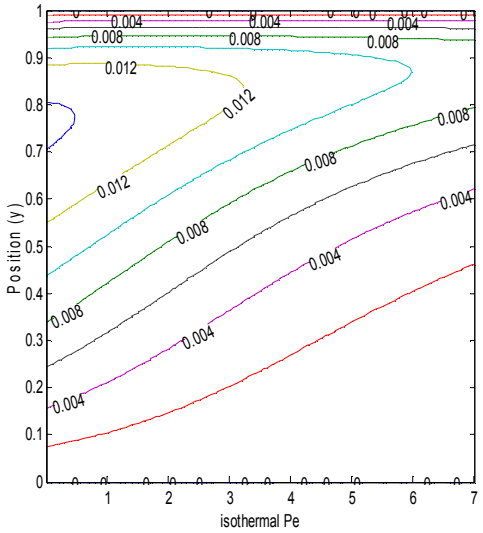

Figure 13: Contour graph of temperature θ(y) at various values of Pe with Re = 5.0, Br = 0.3, M = 1.0, Da = 0.1 (isothermal) for equation (12)

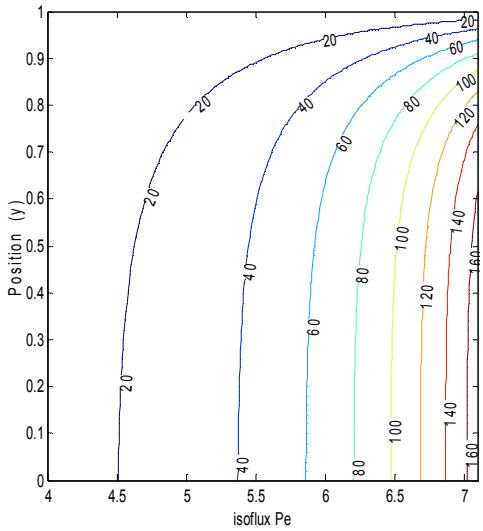

Figure 14: Contour graph of temperature θ(y) at various values of Pe with Re = 5.0, Br = 0.3, M = 1.0, Da = 0.1 (isoflux) for equation (12)

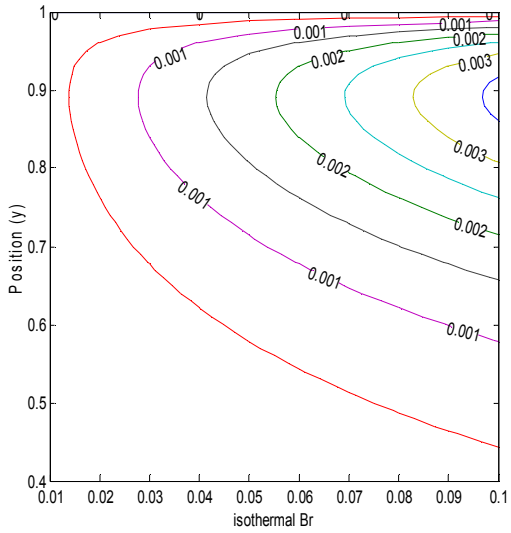

Figure 15: Contour graph of temperature θ(y) at various values of Br with Re = 5.0, Pe = 7.1, M = 1.0, Da = 0.1 (isothermal) for equation (12)

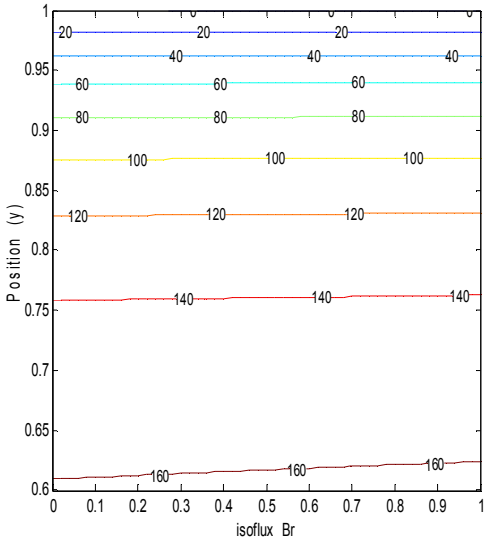

Figure 16: Contour graph of temperature θ(y) at various values of Br with Re = 5.0, Pe = 7.1, M = 1.0, Da = 0.1 (isoflux) for equation (12)

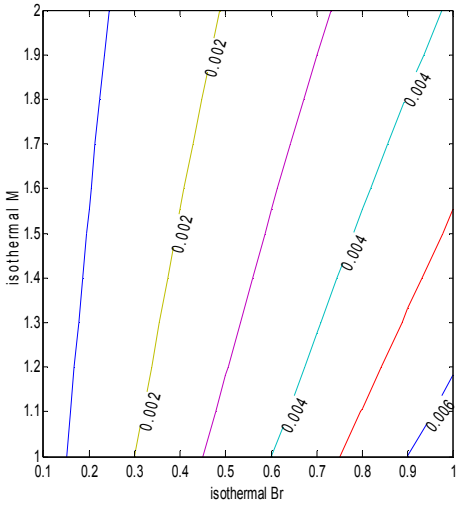

Figure 17: Contour graph of temperature θ(y) at various values of Br and M with Re = 5.0, Pe = 7.1, Da = 0.1, y = 0.5 (isothermal) for equation (12)

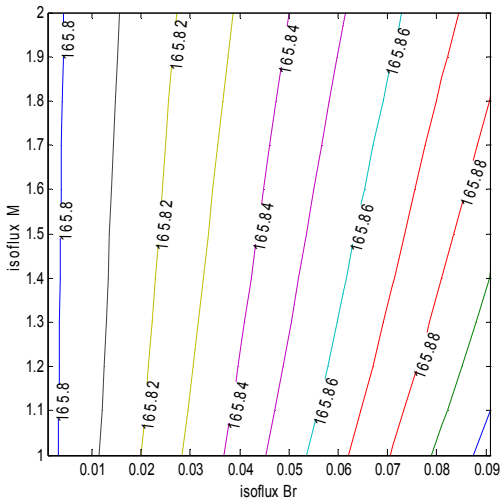

Figure 18: Contour graph of temperature θ(y) at various values of Br and M with Re = 5.0, Pe = 7.1, Da = 0.1, y = 0.5 (isoflux) for equation (12)

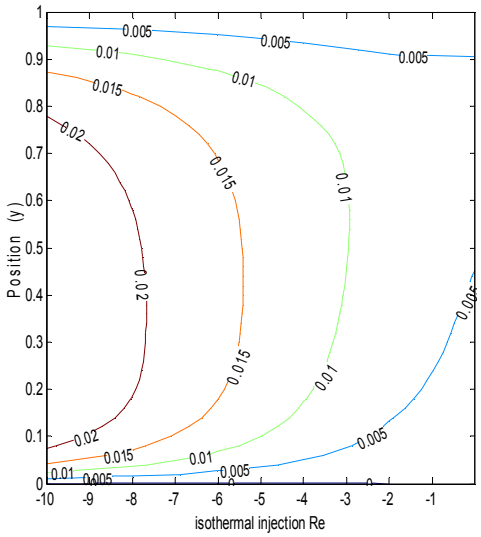

Figure 19: Contour graph of temperature θ(y) at various values of injection Re with Br = 0.3, Da = 0.1, Pe = 7.1, M = 1.0 (isothermal) for equation (12)

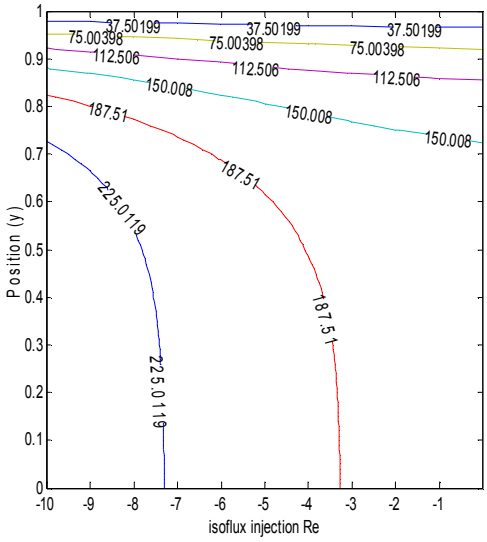

Figure 20: Contour graph of temperature θ(y) at various values of injection Re with Br = 0.3, Da = 0.1, Pe = 7.1, M = 1.0 (isoflux) for equation (12)

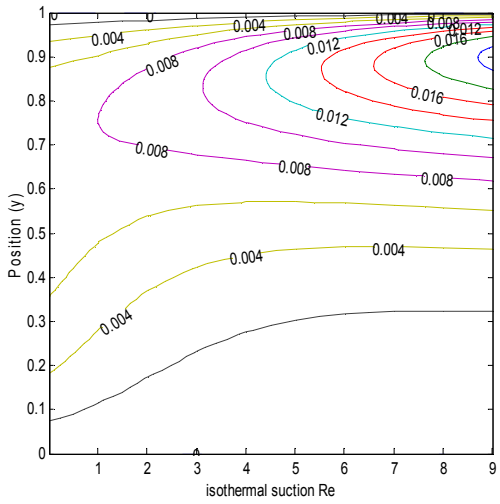

Figure 21: Contour graph of temperature θ(y) at various values of suction Re with Br = 0.3, Da = 0.1, Pe = 7.1, M = 1.0 (isothermal) for equation (12)

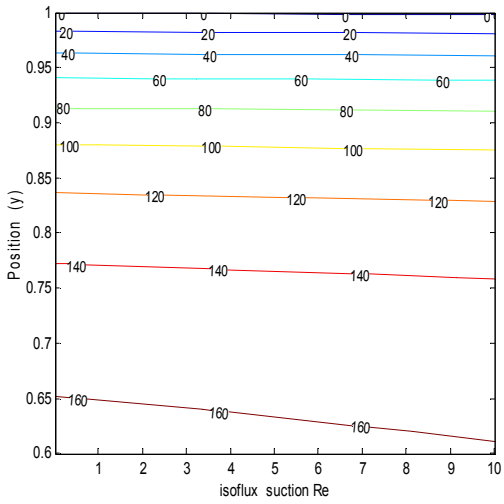

Figure 22: Contour graph of temperature θ(y) at various values of suction Re with Br = 0.3, Da = 0.1, Pe = 7.1, M = 1.0 (isoflux) for equation (12)

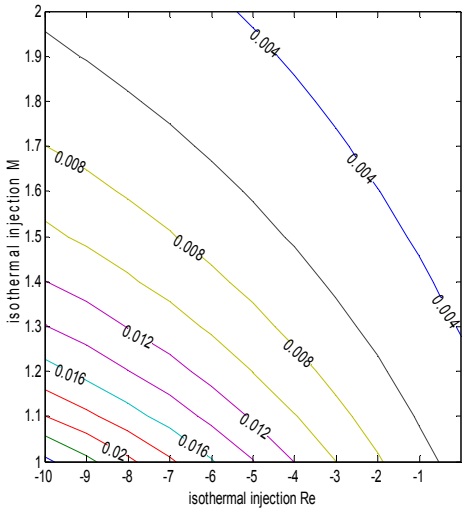

Figure 23: Contour graph of temperature θ(y) at various values of injection Re and M with Br = 0.3, Da = 0.1, Pe = 7.1, y = 0.5, (isothermal) for equation (12)

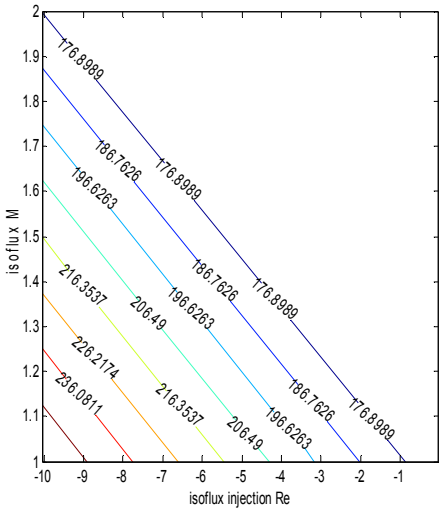

Figure 24: Contour graph of temperature θ(y) at various values of injection Re and M with Br = 0.3, Da = 0.1, Pe = 7.1, y = 0.5, (isoflux) for equation (12)

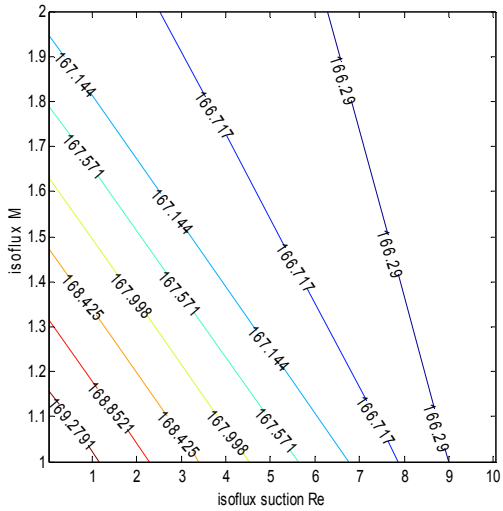

Figure 25: Contour graph of temperature θ(y) at various values of suction Re and M with Br = 0.3, Da = 0.1, Pe = 7.1, y = 0.5, (isoflux) for equation (12)

The IISTE is a pioneer in the Open-Access hosting service and academic event management. The aim of the firm is Accelerating Global Knowledge Sharing.

More information about the firm can be found on the homepage:
http://www.iiste.org

CALL FOR JOURNAL PAPERS

There are more than 30 peer-reviewed academic journals hosted under the hosting platform.

Prospective authors of journals can find the submission instruction on the following page: http://www.iiste.org/journals/ All the journals articles are available online to the readers all over the world without financial, legal, or technical barriers other than those inseparable from gaining access to the internet itself. Paper version of the journals is also available upon request of readers and authors.

MORE RESOURCES

Book publication information: http://www.iiste.org/book/

Academic conference: http://www.iiste.org/conference/upcoming-conferences-call-for-paper/

IISTE Knowledge Sharing Partners

EBSCO, Index Copernicus, Ulrich's Periodicals Directory, JournalTOCS, PKP Open Archives Harvester, Bielefeld Academic Search Engine, Elektronische Zeitschriftenbibliothek EZB, Open J-Gate, OCLC WorldCat, Universe Digtial Library , NewJour, Google Scholar